Comparative study of the catalytic properties of ferrierite zeolite exchanged with alkaline earth metals in the skeletal isomerization of n-butene

P. Cañizares * and A. Carrero

Department of Chemical Engineering, Faculty of Chemistry, University of Castilla-La Mancha, Campus Universitario s/n. 13004, Ciudad Real, Spain
E-mail: pcanizar@inqu-cr.uclm.es

Received 21 September 1999; accepted 6 December 1999

Ferrierite zeolites ion exchanged with alkaline earth cations (Mg^{2+}, Sr^{2+}, Ba^{2+}) were prepared and examined as catalysts for the skeletal isomerization of 1-butene. The samples were characterized by XRD, atomic absorption spectroscopy, ammonia TPD, FT-IR, BET/pore size distribution and pyridine chemisorption. The acidity studies indicated that acid strength increases in the order $H^+ > Mg^{2+} > Sr^{2+} > Ba^{2+}$, therefore, the number of weak acid sites follows the opposite trend. At the same time, Brønsted acid sites associated with protons disappear and the number of Lewis acid sites increases with metal content. The presence of bulky cations like Mg^{2+}, Sr^{2+}, Ba^{2+} leads to a slight reduction of surface area and pore size. Ferrierites containing magnesium exhibit the highest isobutene yield. Lewis acid sites are responsible for improvement in catalyst stability as well as suppression of coke formation.

Keywords: skeletal isomerization, isobutene, ferrierite, alkaline earth cations

1. Introduction

Isobutene is an important raw material for the production of methyl *tert*-butyl ether (MTBE) which is widely used as a major octane-enhancer in reformulated gasoline. However, the current supply of isobutene from the catalytic cracking of petroleum is not sufficient to meet the increasing demand of MTBE. Therefore, considerable interest has been devoted to finding a new isobutene source via skeletal isomerization of n-butene [1].

Monomolecular [2,3] and bimolecular [4,5] reaction paths are considered to be possible ways for the conversion of n-butene to isobutene. n-butene molecules activated on acid sites can be solely isomerized through protonated cyclopropane rings [6] or carbenium ions [1] by monomolecular reaction. In bimolecular reactions, dimerized butenes isomerize to suitable octene isomers and are cracked to isobutene and by-products according to figure 1. It should be desirable to suppress or at least minimize side reactions; this objective can be achieved by adjusting the pore size and acid properties of the catalysts.

A number of catalysts such as halogenated aluminas, zeolites and related molecular sieves [7] have been tested for their effectiveness in n-butene skeletal isomerization. These studies have shown that medium pore zeolites (10 MR windows) like ferrierite are significantly more selective than amorphous solids and large pore zeolites. One of the reasons for the superior catalytic behavior of such zeolites comes from their constrained channel system which may depress side reactions such as oligomerization, cracking and H-transfer enhancing the skeletal isomerization of n-butene into isobutene [8].

Furthermore, if pore structure is an important parameter for achieving high isobutene selectivities, there are other factors, such as the acidity of the catalyst, that may strongly influence the product selectivity. As mentioned above, there are secondary reactions like n-butene oligomerization which forms octenes that are prompt to crack leading to butylenes but mainly to propylene and pentenes [9]. It is generally accepted that the acid strength required for these reactions decreases in the order: cracking $\approx$ oligomerization $>$ skeletal isomerization [10]. According to this, strong acid sites will promote undesired reactions, while weak acid sites will be more selective towards

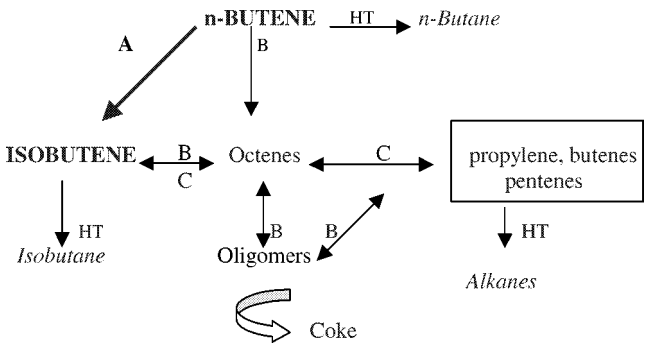

Figure 1. Scheme of skeletal isomerization of n-butene through a monomolecular and a bimolecular reaction mechanism. A: skeletal isomerization, B: dimerization or oligomerization, HT: hydrogen transfer, C: cracking.

* To whom correspondence should be addressed.

skeletal isomerization [11]. Besides, Cheng et al. [12] and Seo et al. [13] suggest that the selectivity to isobutene in the skeletal isomerization varies according to type of acid site. On fluorine-modified alumina, the reaction proceeds on Brønsted acid sites through a bimolecular path, but the monomolecular reaction proceeds on Lewis acid sites. The increase in the selectivity of fluorine modification was explained by the increase of the number of Lewis acid sites under the assumption of monomolecular skeletal isomerization.

In a previous work [14], ZSM-22 type zeolite was ion exchanged with various cations and examined as catalyst in the skeletal isomerization of 1-butene to isobutene. The order of the catalysts with respect to the yield for isobutene was proportional to the ratio of Lewis acidity to Brønsted acidity, as well as suppression of coke formation. The sample with the best catalytic behavior was Mg-ZSM-22. Furthermore, Li et al. [15] verified the decrease in the Brønsted acidity and a slight increase in the number of Lewis acid sites in Mg-ZSM-5 type zeolite prepared via a solid-state reaction of HZSM-5 with magnesium chloride at 327 °C.

In this work, the strength of the Brønsted acid sites of the ferrierite zeolite with a given Si/Al ratio is decreased by exchanging part of the protons associated with the framework aluminium (Si–OH–Al bridges) with other divalent cations such as Mg^{2+}, Sr^{2+}, Ba^{2+}. Thus, we have been able to compare the isobutene yield and selectivity in the skeletal isomerization of n-butene over ferrierite zeolites having different type, number and strength of acid sites. In addition, the presence of cations with larger size than H^+ will reduce the free space in the pores and in the channels of the ferrierite.

2. Experimental

2.1. Catalyst preparation

The ferrierite sample (Si/Al = 20) was prepared by hydrothermal methods using piperidine as a structure-directing template according to [16]. H-FER was obtained by conventional ion exchange with 1 M NH_4Cl aqueous solution two times (80 °C for 12 h), dried and calcined at 550 °C for 12 h.

The H-FER zeolite was then back exchanged with cations such as Mg^{2+}, Sr^{2+}, Ba^{2+} in 0.5 M aqueous metal chloride solutions at 80 °C for 12 h several times, in order to obtain different metal content. Finally, the resultant metal–FER was filtered, washed with deionized water until free of chloride ions, dried and calcined at 550 °C.

2.2. Characterization of catalysts

The crystallinity of the prepared catalysts was confirmed by XRD (Philips PW-1700 powder diffractometer) analysis using a monochromatic Cu Kα radiation and a nickel filter.

In order to quantify the metal (Mg^{2+}, Sr^{2+}, Ba^{2+}) content of the ferrierite samples, atomic absorption spectroscopy (AAS) measurements were made using a Varian 220 FS spectrophotometer. The samples were previously dissolved in hydrofluoric acid and diluted to the interval measurement.

Fourier transform infrared (FT-IR) spectra were recorded on a Perkin–Elmer 16-PC spectrophotometer at a resolution of 4 cm^{-1} by using either KBr pellets or self-supporting wafers. Pyridine chemisorption experiments were done on self-supported wafers in an *in situ* IR cell. The sample was dehydrated under vacuum at 400 °C for 16 h followed by adsorption of pyridine vapor at room temperature for 15 min. After reaching equilibrium, the samples were outgassed at 150 °C under vacuum and the FT-IR spectra were recorded in the 1400–1600 cm^{-1} region.

Pore size distribution was determined by nitrogen adsorption and desorption data acquired on a Micromeritics ASAP 2010 adsorptive and desorptive apparatus. The samples were evacuated under a vacuum of 10^{-5} Torr at 350 °C for over 10 h before measurement. The Horvath–Kawazoe method was used to determine the distribution of micropores.

Temperature-programmed desorption (TPD) experiments were done on a Micromeritics TPD/TPR 2900. The sample was first heated from room temperature to 550 °C at a rate of 15 °C/min and then soaked at 550 °C for 30 min under a flow of 100 ml/min ultrapure helium. The system was then cooled to 180 °C and maintained for 30 min. Ammonia was then flowed over the sample for 15 min. The sample was then purged with helium for 1 h in order to eliminate physisorbed species. The temperature was ramped at 15 °C/min from 180 to 560 °C and TPD data were acquired.

The coke content of the catalysts was determined by combustion in a thermogravimetric analyzer Perkin–Elmer TGA-7. Samples were first heated from 20 to 150 °C in a flow of 20 Nml/min of helium until no weight loss occurred. Then a stream of oxygen was passed through the samples and the temperature was raised to 700 °C at 10 °C/min. The weight loss between 350 and 700 °C was attributed to coke.

2.3. Catalytic experiments

Butene isomerization reactions were carried out in an Autoclave Engineers (BTRS-Jr) microreactor loaded with 250 mg of zeolite catalyst. The reactor was heated from room temperature to 400 °C and maintained during 12 h in a flow of nitrogen of 10 ml/min. Then the nitrogen flow was switched to a mixture of 1-butene and nitrogen (1 : 1 molar ratio). Flow rates of both 1-butene and nitrogen were controlled for obtaining the desired weight hour space velocity (WHSV). Reaction products were analyzed every hour after 10 min time on stream (TOS) by gas chromatography with a Hewlett–Packard 5890 Series II GC equipped with an alumina/KCl capillary column and a flame ionization detector (FID). The results from several experiments show that conversion and isobutene selectivity had an error of $\pm$5%.

Under the whole range of reaction conditions studied, 1-butene isomerizes suddenly to the *cis*- and *trans*-2-butene isomers, so the three linear butenes were considered reactants. Thus, the total conversion (X), selectivity to isobutylene (S_i) and isobutene yield (Y_i) are defined in terms of numbers of carbon atoms:

$$X = \frac{\sum N_i \text{ (except linear butenes)}}{\sum N_i} \times 100 \text{ (\%)},$$

$$S_\mathrm{i} = \frac{N_i}{\sum N_i \text{ (except linear butenes)}(n_i/4)} \times 100 \text{ (\%)},$$

$$Y_\mathrm{i} = X S_\mathrm{i} \text{ (\%)}.$$

In these equations N_i and n_i represent the mole percentage and the number of carbon atoms of each compound, respectively.

3. Results and discussion

3.1. Catalysts characterization

3.1.1. Metal (Mg, Sr, Ba) content and textural properties of ion-exchanged ferrierites

The parent catalyst, H-FER, was ion exchanged with alkaline earth cations (Mg^{2+}, Sr^{2+}, Ba^{2+}). Samples are designed as Me-FER-n, which means that H-FER has been ion exchanged n times with $MeCl_2$ (Me = Mg, Sr, Ba) aqueous solution.

Table 1 shows that the amount of metal measured in the zeolites increases with the number of ion exchanges. By assuming a charge balance between Me^{2+} and AlO_4^-, the atomic ratio Me/Al should be 0.5 at an exchange degree of 100%. As can be seen, for a given number of ion exchanges, for example nine, lower exchange level is achieved in the magnesium sample. This fact can be explained since magnesium has the highest hydrated ratio, in this case solvated water molecules compete with the zeolite framework for magnesium ions. On the opposite, complete replacement of H^+ is achieved after nine ion exchanges with barium chloride solution.

Table 1
Metal (Mg, Sr, Ba) content and textural properties of cation-exchanged ferrierite zeolites.

Sample	Me (Mg, Sr, Ba) (wt%)	Exchange level (%)	BET surf. area (m^2/g)	Pore vol. (cm^3/g)	Pore size[a] (Å)
H-FER	–	–	492.4	0.19	5.40
Mg-FER-7	0.20	17.6	490.0	0.19	5.24
Mg-FER-9	0.27	23.6	481.2	0.18	5.23
Sr-FER-6	0.90	21.3	480.7	0.18	5.18
Sr-FER-9	1.35	31.6	463.1	0.17	5.15
Sr-FER-11	1.83	42.8	444.0	0.17	5.13
Ba-FER-2	1.34	19.4	476.8	0.18	5.17
Ba-FER-6	1.90	27.4	469.6	0.18	5.15
Ba-FER-9	6.02	100.0	404.5	0.17	5.10

[a] Micropore diameter determined using the Horvath–Kawazoe method.

Results of the nitrogen adsorption study over H-FER and ion-exchanged samples are resumed in table 1. The surface area and pore volume of the catalysts decrease with increasing Me content. Futhermore, the adsorption capacity of the Me-FER samples, with similar exchange level, increases in the order Ba-FER-2 < Sr-FER-6 < Mg-FER-7, because the more bulky cation Ba^{2+} (1.34 Å) will most probably cause diffusional limitations to a higher extent than magnesium and strontium ions. Moreover, the introduction of alkaline earth metal ions instead of protons, even with very small ionic radii such as Mg^{2+} (0.66 Å), may also block the intersecting channels leading to a reduction in pore volume and size as expected.

3.1.2. Acidity measurements

FT-IR studies were based on the characterization of Brønsted acid sites by studying the hydroxyl group bands in the 3800–3500 cm^{-1} region with self-supported wafers in an *in situ* IR cell. The sample was previously outgassed under vacuum at 400 °C for 16 h. Ferrierite exhibits two principal bands at ca. 3730 and 3600 cm^{-1} and another one at ca. 3650 cm^{-1} (figure 2). The 3600 and 3650 cm^{-1} bands are assigned to strong and weak acidic hydroxyl groups, respectively [17], while the 3730 cm^{-1} band corresponds to non-acidic silanol groups (terminal groups). We use the 3600 cm^{-1} band corresponding to protonic sites to check that the number of remaining protons decreased when the metal (Mg^{2+}, Sr^{2+}, Ba^{2+}) content increased. A series of solids having decreasing number of acid sites was obtained, as shown in figure 2.

The nature and change of the acid sites of the samples have been examined by chemisorbed pyridine IR studies. For the parent zeolite, H-FER, there were peaks at 1540 and 1490 cm^{-1} and a small peak at 1450 cm^{-1}. This is

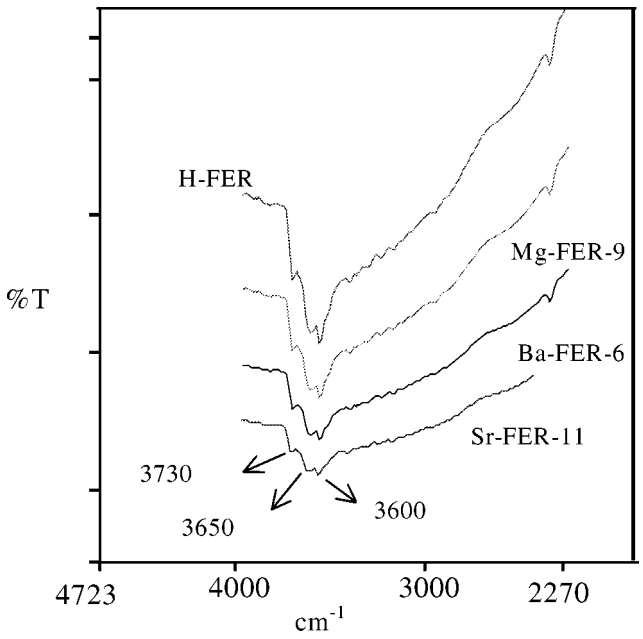

Figure 2. FT-IR spectra of hydroxyl groups for H^+-, Mg^{2+}-, Sr^{2+}- and Ba^{2+}-exchanged ferrierites.

Table 2
Acid properties of cation-exchanged ferrierite zeolites.

Sample	FT-IR	Ammonia TPD			
	Brønsted/	Total acid sites (mmol NH_3/g_{cat})		Desorption temperature (°C)	
	Lewis[a]	Weak	Strong	Weak acid sites	Strong acid sites
H-FER	5.01	0.40	0.55	270	460
Mg-FER-7	2.23	0.45	0.43	270	460
Mg-FER-9	1.96	0.45	0.39	270	442
Sr-FER-9	1.58	0.43	0.37	250	428
Sr-FER-11	1.00	0.44	0.33	250	400
Ba-FER-6	1.82	0.64	0.19	250	390
Ba-FER-9	0.60	0.72		343	

[a] Brønsted/Lewis acid sites ratio was calculated by measuring the peak area at 1540 and 1450 cm^{-1}, pyridine desorption temperature 150 °C.

evidence of a very high concentration of Brønsted acidity and a small amount of Lewis acidity. With addition of alkaline earth ions (Mg^{2+}, Sr^{2+}, Ba^{2+}) to the zeolite, the bands at 1540 and 1490 cm^{-1} reduced, while the band at 1450 cm^{-1} increased due to the existence of $(–Al–O–Me)^+$ species.

Results over H-FER and ion-exchanged samples are presented in table 2. Substitution of protons for divalent cations (Mg^{2+}, Sr^{2+}, Ba^{2+}) causes a decrease of the Brønsted/Lewis acid sites ratio, that is the peak area related with Brønsted acidity is reduced largely while Lewis acidity increases little by little with metal loading.

Temperature-programmed desorption of ammonia allows quantitative determination of the amount and strength of acid sites. Table 2 shows ammonia TPD results for the parent (H-FER) and Me-FER (Me = Mg, Sr, Ba) catalysts.

Desorption of ammonia via increasing the temperature showed two peaks at 270 and 460 °C for H-FER; these peaks correspond to ammonia eluted from weak and strong acid sites, respectively. When H-FER is ion exchanged with alkaline earth metal aqueous solutions, the intensity of the strong acidity peak decreases more and more with increasing metal content, but the weak acidity peak somewhat increases and both peaks shift toward lower temperatures. In other words, the presence of Mg^{2+}, Sr^{2+} and Ba^{2+} ions in cationic positions of ferrierite zeolite instead of protons produces an increase in the weak/strong acid sites ratio, lower acid strength and a decrease in the total number of acid sites. These circumstances lead to important changes in the TPD curves profiles shown in figure 3 corresponding to H-FER and samples exchanged with Mg^{2+}, Sr^{2+} and Ba^{2+}.

These results obtained from catalyst characterization are in agreement with those reported by Kwak et al. [18].

3.2. Catalytic activity of ion-exchanged ferrierites

Ferrierite zeolite in its protonic form was ion exchanged with several cations (Mg^{2+}, Sr^{2+}, Ba^{2+}) and their catalytic activities for the skeletal isomerization of n-butene to isobutylene were examined. Because cation-exchange level increased with the number of ion exchanges (see table 1), all FER zeolites tested in this work were ion exchanged several times with $MeCl_2$ solutions.

Reaction parameters for H-FER and Me (Mg, Sr, Ba)-FER zeolites at the initial stage, $(X, S, Y)_{\text{initial}}$, and after 7 h on stream, $(X, S, Y)_{\text{final}}$ are shown in figure 4. All cation-exchanged samples have higher initial isobutene selectivity than H-FER. The initial selectivity increases with exchange level especially in Mg-FER samples. On the opposite, final selectivity decreases with metal content and all Me-FER samples have values very close one to another.

The Ba-FER-9 sample, with 100% of exchange level, is the most selective at the initial stage of reaction (65.2 versus 55.5% for H-FER). This sample has a NH_3-TPD spectrum without strong acid sites and where Ba^{2+} may limit the space available around the acid sites. Therefore, the formation of bulky branched oligomers and the bimolecular mechanism will be considerably reduced. These facts indicate that initial selectivity is mainly governed by acid strength and space around acid sites and less by the total number of acid sites (see table 2).

Figure 4 also shows an important enhancement in isobutene yield for samples containing strontium and magnesium ions (Mg-FER and Sr-FER). The isobutene yield firstly increases and then passes through a maximum at 20 and 30% of exchange level for Mg-FER and Sr-FER samples, respectively. According to table 1, this exchange percent corresponds to samples designed as Mg-FER-7 and Sr-FER-9, respectively. In contrast, in Ba-FER catalysts the isobutene yield and n-butene conversion are below H-FER and both decrease with exchange percentage. This behavior may be related with lower surface area, acid density and acid strength of barium samples.

From the above paragraphs, we can conclude that the substitution of H^+ ions for divalent cations such as Mg^{2+}, Sr^{2+} and Ba^{2+} in the ferrierite framework, increases the number of Lewis acid sites, while the number of Brønsted acid sites and the acid strength are decreased. Moreover, a slight reduction of pore size is observed. In these sense, by-products development through butene dimerization is more difficult and isobutene formation is favored.

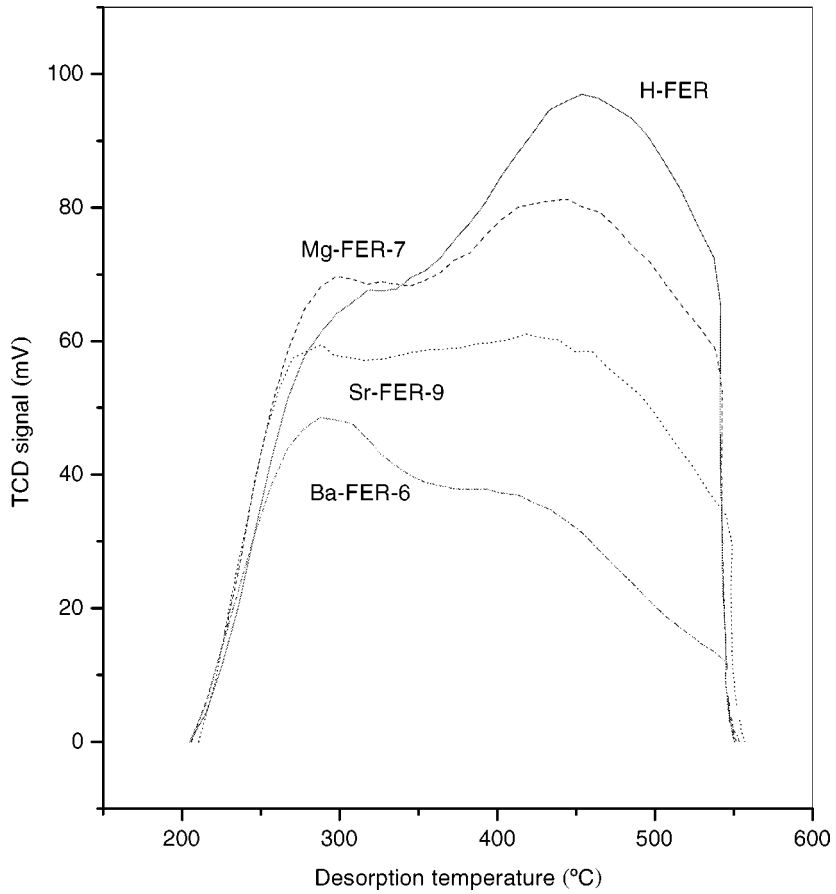

Figure 3. Temperature-programmed desorption of ammonia for H-FER and ferrierite exchanged with alkaline earth metals.

It is known that n-butene conversion decreases with time on stream, while there is a substantial increase in the selectivity to isobutene caused by coke deposits. This enhancement is especially important over H-FER while samples exchanged with alkaline earth cations experiment lower selectivity increase and conversion decrease with coke deposition. These facts are evident since samples exchanged with Mg^{2+} and Sr^{2+} have the same values of initial n-butene conversion as H-FER, but at the end of the run conversion for Mg-FER and Sr-FER catalysts is higher than for H-FER.

There are, however, different opinions regarding the mechanism by which coke deposits might promote the selective formation of isobutene. Poisoning of non-selective acid sites (strong Brønsted acid sites of those located on the external surface) and a reduction of the free space around the acid sites limiting the competitive dimerization reaction have been proposed to explain the effect of coke [19,20]. Moreover, Guisnet et al. [21] proposed that the change from a non-selective to a selective behavior is due to the development of a new isomerization mechanism (pseudo-monomolecular) involving the alkylation of n-butene with a *tert*-butyl cation (formed from isobutene diffusing slowly from the zeolite pores) and cracking of the resulting trimethylpentyl cation in order to explain the increase of isobutene yield observed in ferrierite at short times on stream.

In fact, coke deposits inside the cavities of H-FER were most likely needed in order to produce high selectivity to isobutene. In contrast, since Me-FER samples contain less strong Brønsted acid sites and narrower channels, the modifications by the coke deposits were not as dramatic as for H-FER.

From table 3, it is also observed that catalytic stability was greatly improved by exchanging H-FER zeolite with magnesium and strontium cations. As we have said, it is evident that n-butene conversion decreases with time on stream as a consequence of coke deposition described in the above paragraphs. The amount of coke deposited and $T_{G,max}$ decrease according to H-FER $>$ Mg-FER $>$ Sr-FER $>$ Ba-FER, pointing to the presence of heavier species in the coke formed on the catalyst with strong acid sites. Elsewhere, $T_{G,max}$ is related to coke location [22]; when $T_{G,max}$ is lower, external coke probably increases.

These results are probably related to a reduction in strong Brønsted acid sites, as confirmed by TPD and FT-IR analyses. The strong acid sites of zeolites lead to, not only side reactions, but also rapid coke formation which may be important factors in the deactivation of zeolites in hydrocarbon-related processes. The behavior of barium samples is noticeable since they have less coke amount than the rest of the catalysts but their percentage of deactivation

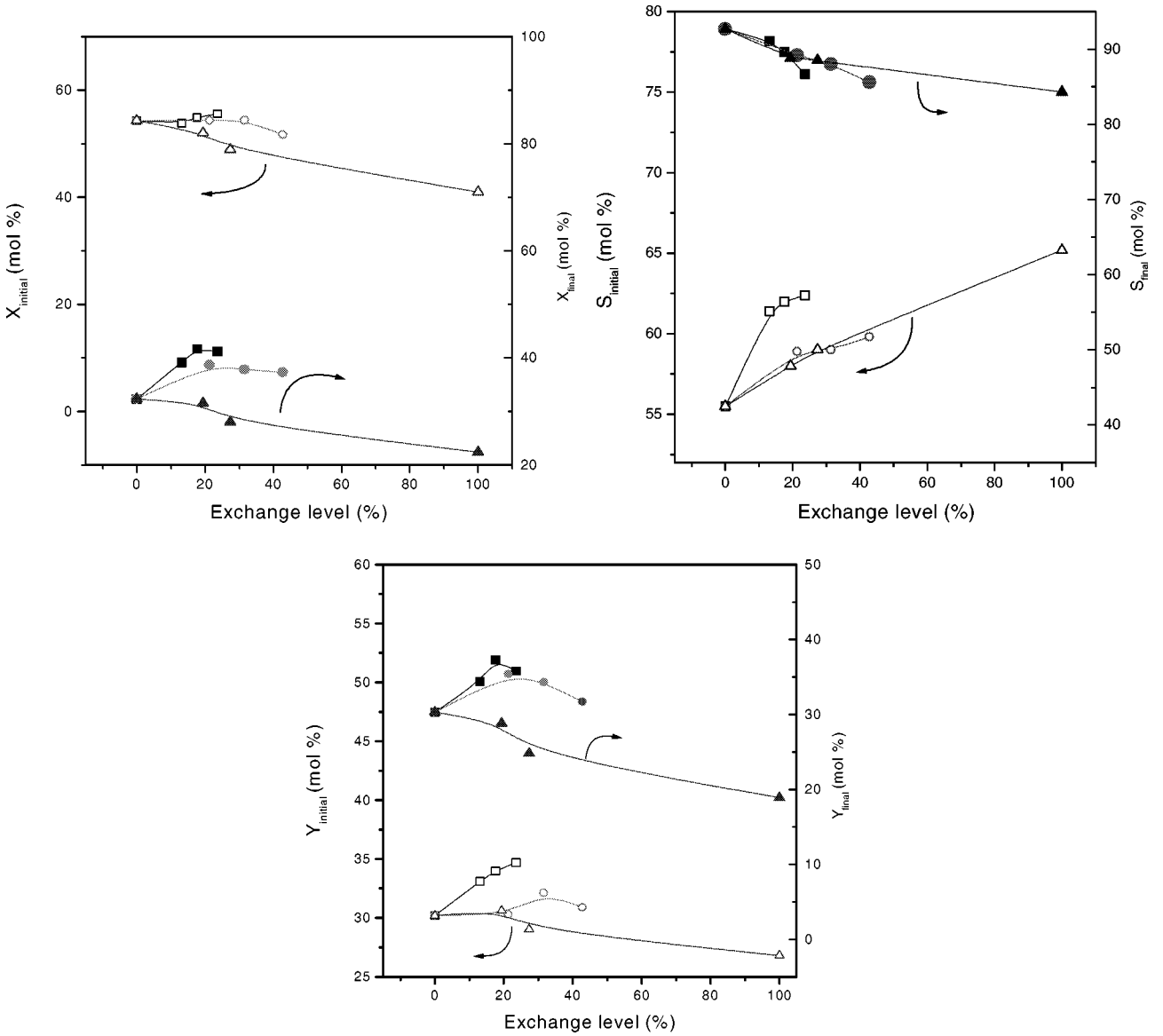

Figure 4. Initial (TOS = 10 min) and final (TOS = 420 min) reaction parameters over H-FER (WHSV for H-FER was adjusted in order to obtain similar levels of conversion) and Me (Mg, Sr, Ba)-FER samples. Influence of the cation nature and exchange level. (T = 400 °C; N_2/n-butene = 1 (v/v); WHSV = 5 h^{-1}.) (□) Mg-FER, (○) Sr-FER and (△) Ba-FER.

is as high as H-FER. This fact may be explained taking into account that on Ba-FER zeolites smaller amounts of coke can produce high deactivation if they are deposited on external acid sites producing pore blocking or topological isolation of the channel structure.

Based on the above results, we have chosen the sample with the best catalytic behavior of each group in order to compare isobutene yield as a function of n-butene conversion (figure 5). Clearly the nature of Me^{2+} cations has a strong influence on isobutene formation. Magnesium samples with surface area as high as H-FER but where part of the strong Brønsted acid sites associated with H^+ has been transformed into weaker Lewis acid sites (see characterization section), are good catalysts for the skeletal isomerization of n-butene. In contrast, barium samples have acid strength and Brønsted acid sites that are so reduced that

Table 3
Coke amount, percentage deactivation and surface area for cation-exchanged ferrierites after 7 h of reaction.

Sample	Coke amount (wt%)	$T_{G,max}$ [a] (°C)	Deactivation[b] (%)
H-FER	5.84	636.5	40.5
Mg-FER-7	5.80	635.2	24.0
Mg-FER-9	5.71	636.9	25.9
Sr-FER-9	5.70	620.6	30.5
Sr-FER-11	5.45	619.2	27.8
Ba-FER-6	5.31	610.5	42.7
Ba-FER-9	4.76	611.0	45.9

[a] Temperature of the differential curve maximum for coke burning.
[b] Ratio of the drop in conversion by deactivation after a 7 h reaction to the initial conversion.

the skeletal isomerization reaction is disfavored and lower isobutene yields are obtained.

Table 4 shows the product distribution in the skeletal isomerization of n-butene over parent (H-FER) and cation-exchanged ferrierites at a time on stream of 10 min. The modification mainly decreases cracking and hydrogen transfer reactions. As just mentioned above, less carbonaceous deposits are formed over Me-FER zeolites, accordingly the formation of hydrogen drops and the selectivity toward alkanes – mainly methane, ethane and propane – is strongly reduced. Since cation-exchanged samples have higher selectivity to C_4 paraffins than to light paraffins (C_1–C_3) it is reasonable to think that strong Brønsted acid sites present on H-FER give cracking reactions in a higher extent than weak Lewis sites belonging to Me-FER samples.

Comparing Ba-FER-6 with the other catalysts, there is an enhancement in pentenes selectivity to the detriment of ethylene and propylene which also confirms that cracking reactions require strong Brønsted acid sites [13,23].

Finally, in order to check the catalytic stability of modified samples, reaction parameters at long times on stream (27 h) for Mg-FER-7 and H-FER are plotted in figure 6. Yields of isobutene for Mg-FER-7 are significantly enhanced compared to those for H-FER. However, only initial selectivity for H-FER is below Mg-FER-7, but as time on stream increases, isobutene selectivity is very close for both

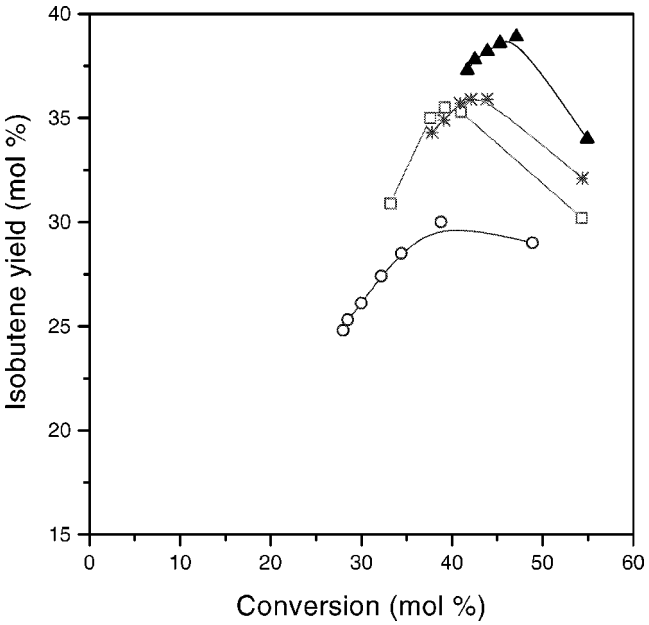

Figure 5. Yields of isobutene over ion-exchanged ferrierites versus n-butene conversion. (□) H-FER, (▲) Mg-FER-7, (∗) Sr-FER-9 and (○) Ba-FER-6. Reaction conditions as in figure 4.

Table 4
Products selectivity (mol%) for n-butene skeletal isomerization over cation-exchanged ferrierites.[a]

Product	Sample			
	H-FER[b]	Mg-FER-7	Sr-FER-9	Ba-FER-6
C_1–C_3 paraf.	10.7	6.2	5.0	2.6
Isobutane	0.8	0.9	1.0	2.5
n-butane	5.0	4.4	4.2	4.5
Ethylene	3.9	3.1	3.8	2.8
Propylene	18.0	16.3	20.1	18.9
Isobutene	55.5	62.0	59.0	59.1
Pentenes	6.1	7.1	6.9	9.6

[a] Reaction conditions: $T = 400\,^{\circ}$C, N_2/n-butene = 1 (v/v), WHSV = 5 h^{-1}, TOS = 10 min.
[b] WHSV for H-FER was adjusted to achieve a similar level of conversion.

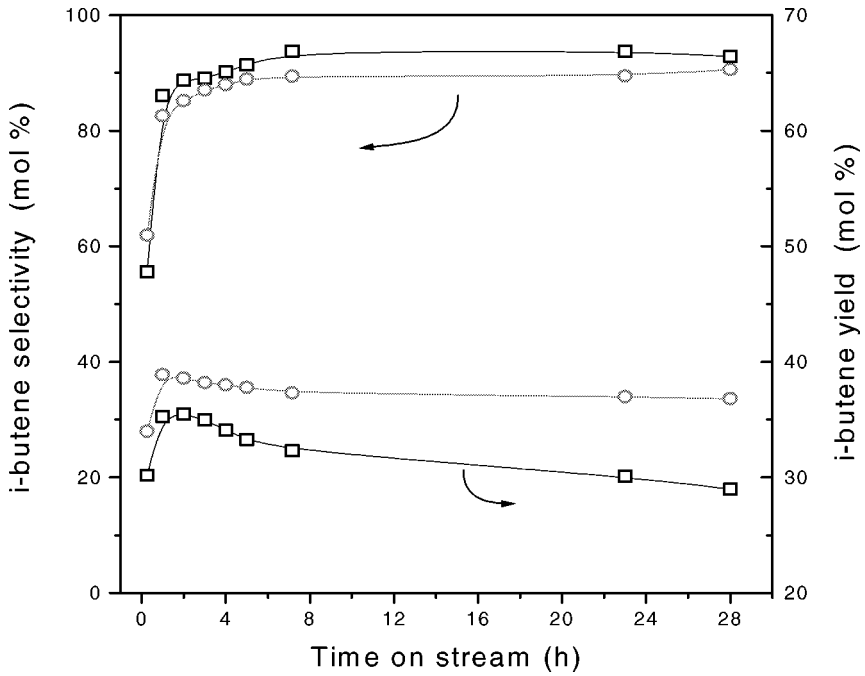

Figure 6. Yield and selectivity for n-butene skeletal isomerization at long times on stream: catalyst stability: (□) H-FER and (○) Mg-FER-7. Reaction conditions as in figure 4.

catalysts. Finally, we can conclude that H^+ exchange for Mg^{2+} improves catalyst stability since the isobutene yield remains almost constant for times on stream higher than 1 h.

4. Conclusions

A series of Me-FER samples was prepared by ion exchange of H-FER with alkaline earth metals such as Mg, Sr and Ba, and tested as catalysts for the skeletal isomerization of 1-butene into isobutene.

The incorporation of alkaline earth cations into ferrierite considerably changes the acidity distribution of the zeolite: total acid sites decrease in number as strong acid sites while weak acid sites are increased. At the same time there is a reduction in the ammonia desorption temperature from both sites, indicating lower values of acid strength. On the other side, Me^{2+} cations generate Lewis acidity with an important reduction in Brønsted acid sites. Textural properties are also modified with decreasing values of BET surface area and pore volume, together with lower values of pore size.

Magnesium-containing samples have the highest isobutylene yield. These catalysts contain acid sites of medium strength and the adequate balance between Brønsted and Lewis acid sites. These acid properties together with a reduction in the space around the acid sites enhanced catalyst stability, decreasing the amount of coke deposited and percentage of deactivation.

As a consequence of weaker acidity, secondary reactions like cracking and hydrogen transfer are impeded and light paraffins selectivity drops while the pentenes/propylene ratio slightly increases.

References

[1] J. Szabo, J. Perrotey, G. Szabo, J.C. Duchet and D. Cornet, J. Mol. Catal. 67 (1991) 79.
[2] G. Seo, H.S. Jeong, S.B. Hongand and Y.S. Uh, Catal. Lett. 36 (1996) 249.
[3] J. Houzvicka and V. Ponec, Ind. Eng. Chem. Res. 36 (1997) 1424.
[4] H.H. Mooiweer, K.P. de Jong, B. Kraushaar-Czarnetzki, W.H.J. Stork and B.C.H. Krutzen, in: *Zeolites and Related Microporous Materials: State of the Art 1994*, Studies in Surface Science and Catalysis, Vol. 84, eds. J. Weitkamp, H.G. Karge, H. Pfeifer and W. Hölderich (Elsevier, Amsterdam, 1994) pp. 2327–2334.
[5] M. Guisnet, P. Andy, N.S. Gnep, E. Benazzi and C. Travers, J. Catal. 158 (1996) 551.
[6] W.-Q. Xu, Y.-G. Yin, S.L. Suib and C.-L. O'Young, J. Catal. 150 (1994) 34.
[7] A.C. Butler and C.P. Nicolaides, Catal. Today 18 (1993) 443.
[8] J.M. Thomas, Sci. Am. April (1992) 112.
[9] V. Ponec and J. Houzvicka, Ind. Eng. Chem. Res. 36 (1997) 1424.
[10] A. Corma and B.W. Wojciechowski, Catal. Rev. Sci. Eng. 24 (1982) 1.
[11] M.W. Simon, W.-Q. Xu, S.L. Suib and C.-L. O'Young, in: *Zeolites and Related Microporous Materials: State of the Art 1994*, Studies in Surface Science and Catalysis, Vol. 84, eds. J. Weitkamp, H.G. Karge, H. Pfeifer and W. Hölderich (Elsevier, Amsterdam, 1994) p. 1671.
[12] Z.X. Cheng and V. Ponec, Appl. Catal. A 118 (1994) 127.
[13] G. Seo, N.-H. Kim, Y.-H. Lee and J.-H. Kim, Catal. Lett. 51 (1998) 101.
[14] S.H. Baeck and W.Y. Lee, Appl. Catal. A 164 (1997) 291.
[15] Y.-G. Li, W.-H. Xie and S. Yong, Appl. Catal. A 150 (1997) 231.
[16] P.A. Jacobs and J.A. Martens, Stud. Surf. Sci. Catal. 33 (1987) 8.
[17] J.C. Vedrine, Y.S. Jin and A. Auroux, Appl. Catal. 37 (1988) 1.
[18] B.S. Kwak, J.H. Jeong and S.H. Park, in: *Progress in Zeolite and Microporous Materials*, Studies in Surface Science and Catalysis, Vol. 105, eds. H. Chon, S.-K. Ihm and Y.S. Uh (Elsevier, Amsterdam, 1997) p. 1423.
[19] P. Mériaudeau, C. Naccache, H.N. Le and T.A. Vu, J. Mol. Catal. A 123 (1997) L1.
[20] R. Byggningsbacka, N. Kumar and L.-E. Lindfors, J. Catal. 178 (1998) 611.
[21] M. Guisnet, P. Andy, Y. Boucheffa, N.S. Gnep, E. Benazzi and C. Travers, Catal. Lett. 50 (1998) 159.
[22] A. Lucas, P. Cañizares, A. Durán and A. Carrero, Appl. Catal. 156 (1997) 299.
[23] B.S. Kwak and J. Sung, Catal. Lett. 53 (1998) 125.